Robotica (1988) volume 7, pp 191–198

Compliance control and stability analysis of cooperating robot manipulators

H. Kazerooni

Mechanical Engineering Department, 111 Church Street SE University of Minnesota Minneapolis, Minnesota, 55455 (USA)

(Received in Final Form: July 29, 1988)

SUMMARY

The work presented here is the description of the control strategy of two cooperating robots. A two-finger hand is an example of such a system. The control method allows for position control of the contact point by one of the robots while the other robot controls the contact force. The stability analysis of two robot manipulators has been investigated using unstructured models for dynamic behavior of robot manipulators. For the stability of two robots, there must be some initial compliance in either robot. The initial compliance in the robots can be obtained by a non-zero sensitivity function for the tracking controller or a passive compliant element such as an RCC.

KEYWORDS: Compliance; Stability analysis; Cooperating robots; Control strategy.

INTRODUCTION

The paper develops the essential rules in stability analysis of two cooperating robots. We assume the robots initially have some type of independent tracking capabilities. This assumption permits us to extend the control analysis to cover industrial robot manipulators in addition to research robots. The tracking capability allows each robot to follow its individual command independently when it is not constrained by each other. Once the robots come in contact with each other, the contact force between the two robots is fed back to one of the robots to develop compliance.[1–4] The compliance in one of the robots allows for control of the contact force, while the other robot governs the position of the contact point. A stability bound has been developed on the size of the force feedback gain to stabilize the closed loop system of both robots. The stability analysis has been investigated using unstructured models for the dynamic behavior of the robot manipulators. This unified approach of modeling robot dynamics is expressed in terms of sensitivity functions as opposed to the Lagrangian approach. It allows us to incorporate the dynamic behavior of all the elements of a robot manipulator (i.e. actuators, sensors and the structural compliance of the links) in addition to the rigid body dynamics.[4]

DYNAMIC MODEL OF THE ROBOT

In this section, a general approach will be developed to industrial and research robot manipulators having positioning (tracking) controllers. The fact that most industrial manipulators already have some kind of positioning controller is the motivation behind our approach. Also, a number of methodologies exist for the development of robust positioning controllers for direct and non-direct robot manipulators.[5]

In general, the end-point position of a robot manipulator that has a positioning controller is a dynamic function of its input trajectory vector, e, and the external force, f. Let G and S be two functions that describe the robot end-point position, y, in a gobal coordinate frame.* (f is measured in the global coordinate frame also.)

$$y = G(e) + S(f) \tag{1}$$

The motion of the robot end-point in response to imposed forces, f, is caused either by structural compliance in the robot or by the compliance of the positioning controller. In a simple example, if a Remote Center Compliance (RCC) with a linear dynamic behavior is installed at the endpoint of the robot, then S is equal to the reciprocal of stiffness (impedance in the dynamic sense) of the RCC. Robots with tracking controllers are not infinitely stiff in response to external forces (also called disturbances). Even though the positioning controllers of robots are usually designed to follow the trajectory commands and reject disturbances, the robot end-point will move somewhat in response to imposed forces on it. S is called the sensitivity function and it maps the external forces to the robot end-point position. For a robot with a "good" positioning controller, S in a mapping with small gain. No assumption on the internal structures of $G(e)$ and $S(f)$ are made. Figure 1 shows the nature of the mapping in equaton (1).

Figure 2 shows one possible example of internal structure of the model represented by equation (1). The

* The assumption that linear superposition (in equation (1)) holds for the effects of f and e is useful in understanding the nature of the interaction between two robots. This interaction is in a feedback form and will be clarified with the help of Figure 3. We will note later that the results of the nonlinear analysis do not depend on this assumption, and one can extend the obtained results to cover the case when $G(e)$ and $S(f)$ do

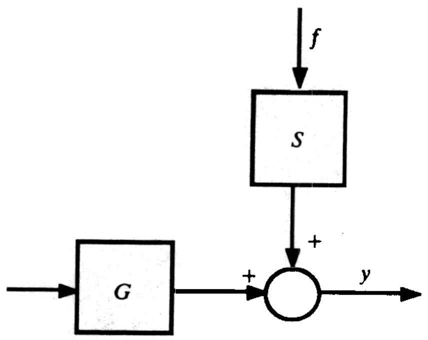

Fig. 1. The dynamics of the robot. All the operators of the block diagrams are unspecified and may be transfer function matrices or time domain input–output relationships.

robot open loop dynamic equation is $M(\theta)\ddot{\theta} + C(\theta, \dot{\theta}) + G_r(\theta) = \tau + J_c^T f$ where $M(\theta)$, $C(\theta, \dot{\theta})$, $G_r(\theta)$ and J_c are the inertia matrix, coriolis, gravity forces and the Jacobian. With the help of two mappings, T_1 and T_2, we define θ_d and θ as the desired position and the actual position of the robot in the joint coordinate frame. P1 and P2 are computer programs that calculte the best estimated values of nonlinear terms in robot dynamics. K_p and K_v are appropriate position and velocity gains to stabilize the system (5). The system in Figure 2 with two inputs (e and f), and one output, y, can be represented by block diagram of Figure 1. Note that equation (1) is not necessarily restricted to be composed of the elements of the block diagram of Figure 2; the block diagram of Figure 2 is given here as an example to show how one can actually model a robot with equation (1). Also note that the model given by equation (1) is not meant to be valid for controller design; it is only for the purpose of stability analysis.

Equation (1) represents an input/output functional relationship. This unified approach of modeling allows us to incorporate the dynamic behavior of all the elements of the robot. We believe that there may be enough components in the robot itself that rigid body dynamics (as given in Figure 2) is not sufficient for modeling. In fact, in many industrial hydraulic robots, the actuators and the servovalves dynamics dominate the total dynamic behavior of the robots. We try to avoid using structured dynamic models such as first or second order transfer functions as general representations of the dynamic behavior of the components of the robot (e.g. servovalves in the hydraulic robots and the gear stiffness in the non-direct drive systems). Throughout this paper we assume the robot dynamic behavior is given by equation (1) where $G(e)$ and $S(f)$ can be computed experimentally or analytically from the closed loop block diagram similar to the one given in Figure 2. A robot with good tracking capability has a small gain for S (rejects all the forces) while a robot with a weak tracking capability has a large gain for S. In fact, an open loop robot—which has the weakest tracking capability-can be modeled with the largest gain on S. If we define an open loop robot as a system with very small feedback gain (K_p and $K_v \to 0$ in the case of Figure 2) then equation (1)—with a large gain for S – can be used to model the open loop robots also. Therefore we define $G(e)$ and $S(f)$ as stable, nonlinear operators in L_p-space to represent the dynamic behavior of not only the closed loop robots but also the open loop (in the sense of above definition) robots. $G(e)$ and $S(f)$ are such that $G\colon L_p^n \mapsto L_p^n$, $S\colon L_p^n \mapsto L_p^n$ and also there exist constants α_G, β_G, α_S and β_S such that $\|G(e)\|_p \le \alpha_G \|e\|_p + \beta_G$ and $\|S(f)\|_p \le \alpha_S \|f\|_p + \beta_S$. α_S is called the gain of operator S.

A similar modeling method can be given for analysis of the linearly treated robots.* The transfer function matrices, G and S in equation (2) are defined to describe the dynamic behavior of a linearly treated robot manipulator with positioning controller.

$$y(j\omega) = G(j\omega)e(j\omega) + S(j\omega)f(j\omega) \tag{2}$$

In equation (2), S is called the sensitivity transfer function matrix and it maps the external forces to the end-point position. $G(j\omega)$ is the closed loop transfer function matrix that maps the input trajectory vector, e, to the robot end-point position, y. For a robot with a "good" positioning controller, within the closed loop bandwidth $S(j\omega)$ is "small" in the singular value sense, while $G(j\omega)$ is approximately a unity matrix. We define

* Throughout this paper, for the benefit of clarity, we develop the frequency domain theory for linearly treated robots in parallel with the nonlinear analysis.

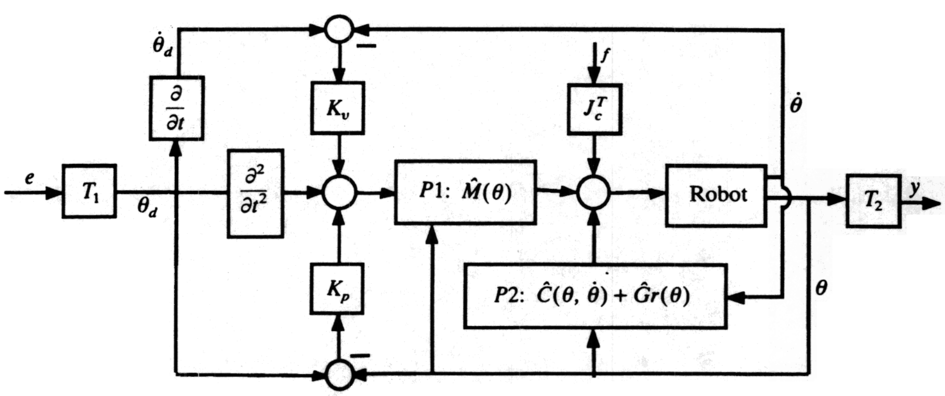

Fig. 2. An example to develop positioning controller for a robot manipulator with rigid body dynamics. $M(\theta)$, $C(\theta, \dot{\theta})$ and $G_r(\theta)$ are the estimated values (5).

S^{-1} as inverse function of the S function:

$$f = S^{-1}(y - G(e)) \tag{3}$$

DYNAMICS OF TWO ROBOTS

Suppose two manipulators with dynamic equation (1) are in contact with each other. Equations (4) and (5) represent the entire dynamic behavior of two interacting robots.

$$y_1 = G_1(e_1) + S_1(f_1) \tag{4}$$

$$f_2 = S_2^{-1}(y_2 - G_2(e_2)) \tag{5}$$

where

$$y_1 = y_2 \quad \text{and} \quad f_1 = -f_2$$

Figure 3 shows the block diagram of the interaction of two robots. Note that the blocks in Figure 3 are in general non-linear operators, however, in the linear case one can treat these blocks as transfer function matrices. If all the operators of the block diagram in Figure 3 were transfer function matrices, then the contact force, f_2, could be calculated from equation (6).

$$f_2 = (S_1 + S_2)^{-1}(G_1 e_1 - G_2 e_2) \tag{6}$$

Equation 6 motivates the block diagram of Figure 4 for representation of the contact force in the system where V_1 and V_2 are given by equations (7) and (8).

$$V_1 = (S_1 + S_2)^{-1} G_1 \tag{7}$$

$$V_2 = (S_1 + S_2)^{-1} G_2 \tag{8}$$

$$f_2 = V_1 e_1 - V_2 e_2 \tag{9}$$

We assume Figure 4 is valid for representation of the non-linear case also. In other words, considering equations (4) and (5) as original equations for dynamic behavior of the robots, one can arrive at operators V_1 and V_2 to show the contributions of e_1 and e_2 on the contact force. We assume V_1 and V_2 are two L_p-stable operators, in other words $V_1(e_1)\colon L_p^n \mapsto L_p^n$ and $V_2(e_2)\colon L_p^n \mapsto L_p^n$ and also there exist positive scalars α_1, α_2, β_1 and β_2 such that:

$$\|V_1(e_1)\|_p \le \alpha_1 \|e_1\|_p + \beta_1 \tag{10}$$

$$\|V_2(e_2)\|_p \le \alpha_2 \|e_2\|_p + \beta_2 \tag{11}$$

See Appendix A for some definitions on the L_p stability.

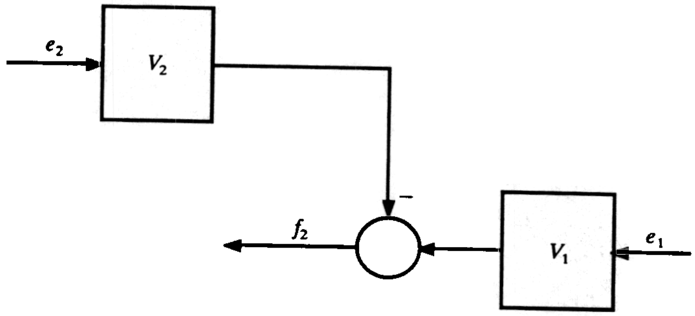

Fig. 4. V_1 and V_2 describe the contributions of both inputs, e_1 and e_2.

THE CLOSED-LOOP SYSTEM FOR TWO ROBOTS

The control architecture in Figure 5 shows how we develop compliancy in the system. H_2 is a compensator to be designed for the second robot. The input to this compensator is the contact force, f_2. The compensator output signal is being added vectorially with the input command vector, r_2, resulting in the error signal, e_2 for the second robot manipulator. One can think of this architecture as a system that allows the second robot to "control" the force and the first robot to "control" the position.

There are two feedback loops in the system; the first loop (which is the natural feedback loop), is the same as the one shown in Figure 3. This loop shows how the contact force affects the robots in a natural way when two robots are in contact with each other. The second feedback loop is the controlled feedback loop.

If two robots are not in contact, then the dynamic behavior of each robot reduces to the one represented by equation (1) (with $f = 0$), which is a simple tracking system. When the robots are in contact with each other, then the contact forces and the end-point positions of robots are given by f_1, f_2, y_1 and y_2 where the following equation are true:

$$y_1 = G_1(e_1) + S_1(f_1) \tag{12}$$

$$f_2 = S_2^{-1}(y_2 - G_2(e_2)) \tag{13}$$

$$y_1 = y_2 \tag{14}$$

$$f_1 + f_2 = 0 \tag{15}$$

$$e_2 = r_2 + H_2(f_2) \tag{16}$$

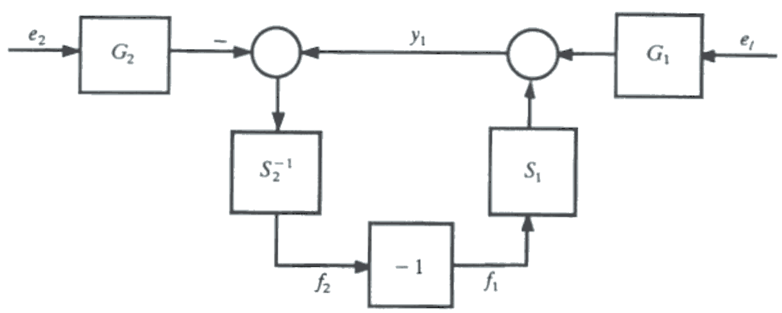

Fig. 3. Interaction of two robots.

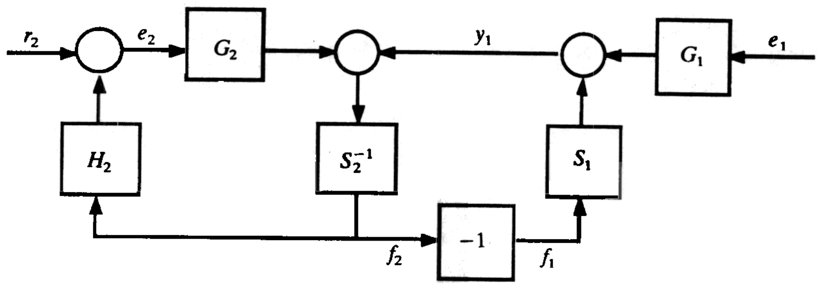

Fig. 5. The closed-loop system, the first robot controls the position and the second robot controls the force.

If all the operators are considered linear transfer function matrices, then:

$$f_2 = (S_1 + S_2 + G_2H_2)^{-1}(G_1e_1 - G_2r_2) \tag{17}$$

We plan to choose a class of compensators, H_2, to control the contact force with the input command r_2. This controller must also guarantee the stability of the closed-loop system shown in Figure 5. Note that the robot sensitivity functions and the electronic compliancy, G_2H_2, add together to form the total sensitivity of the system. If $H_2 = 0$, then only the sensitivity functions of two robots add together to form the compliancy of the system. By closing the loop via H_2, one can not only add to the total sensitivity but also shape the sensitivity of the system.

When two robots are not in contact with each other, the actual end-point position of each robot is almost equal to its input trajectory command governed by equation (1) (with $f = 0$). When the robots are in contact with each other, the contact force on the second robot follows r_2 according to equations (12)–(16). The input command vector, r_2, is used differently for the two categories of maneuverings of the second robot; as an input trajectory command in unconstrained space (equation (1) with $f = 0$) and as a command to control the force in constrained space.

STABILITY

The objective of this section is to arrive at a sufficient condition for stability of the system shown in Figure 5. This sufficient condition leads to the introduction of a class of compensators, H_2, that can be used to develop compliancy for the class of robot manipulators that have positioning controllers. The following theorem (Small Gain Theorem)[6,7] states the stability condition of the closed-loop system shown in Figure 6. A corollary is given to represent the size of H_2 to guarantee the stability of the system.

If condition I, II and III hold:

I. V_1 and V_2 are L_p-stable operators, that is $V_1(e_1)$: $L_p^n \mapsto L_p^n$ and $V_2(e_2)$: $L_p^n \mapsto L_p^n$ and:

$$\text{a) } \|V_1(e_1)\|_p \le \alpha_1 \|e_1\|_p + \beta_1$$

$$\text{b) } \|V_2(e_2)\|_p \le \alpha_2 \|e_2\|_p + \beta_2$$

II. H_2 is chosen such that mapping $H_2(f_2)$ is L_p-stable that is

$$\text{a) } H_2(f_2)\text{: } L_p^n \mapsto L_p^n \tag{20}$$

$$\text{b) } \|H_2(f_2)\|_p \le \alpha_3 \|f_2\|_p + \beta_3 \tag{21}$$

III. and $\alpha_2\alpha_3 < 1$

then the closed loop system in Figure 6 is stable. The proof is given in Appendix A. The following corollary develops a stability bound if H_2 is selected as a linear transfer function matrix.

Corollary

The key parameter in the proposition is the size of $\alpha_2\alpha_3$. According to the proposition, to guarantee the stability of the system, H_2 must be chosen such that $\alpha_2\alpha_3 < 1$. If H_2 is chosen as a linear operator (the impulse response) while all the other operators are still nonlinear, then:

$$\|H_2(f_2)\|_p \le \gamma \|f_2\|_p \tag{23}$$

where

$$\gamma = \sigma_{\max}(N)$$

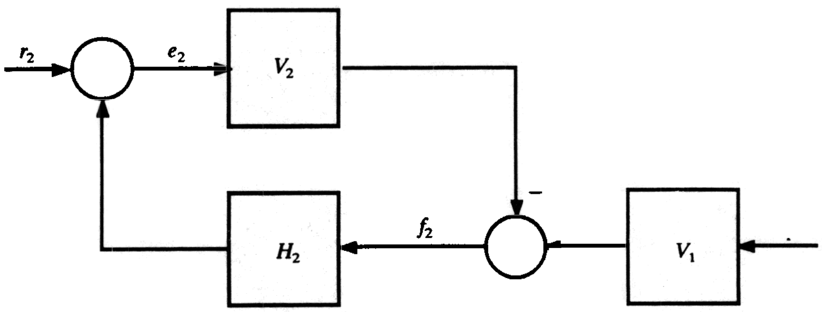

Fig. 6. Two manipulators with force feedback compensator.

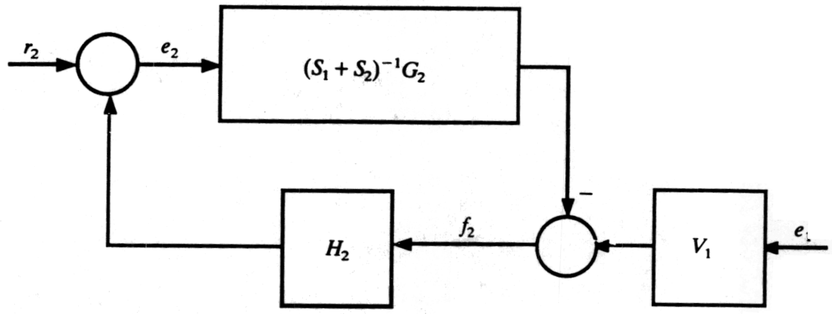

Fig. 7. In the Linear Case, $V_2=(S_1+S_2)^{-1}G_2$ and $V_1=(S_1+S_2)^{-1}G_1$

σ_{max}* indicates the maximum singular value, and N is a matrix whose ijth entry is $\|H_2(\cdot)_{ij}\|_1$. In other words, each member of N is the L_1 norm of each corresponding member of $H_2(\cdot)$ (pulse response). Considering inequality 23, the third stability condition, inequality 22, can be rewritten as:

$$\gamma\alpha_2<1 \tag{25}$$

To guarantee the closed loop stability, $\gamma\alpha_2$ must be smaller than unity, or, equivalently:

$$\gamma<\frac{1}{\alpha_2} \tag{26}$$

To guarantee the stability of the closed loop system, H_2 must be chosen such that its "size" is smaller than the reciprocal of the "gain" of the forward loop mapping in Figure 6. Note that γ represents a "size" of H_2 in the singular value sense.

When all the operators are linear transfer function matrices one can use Multivariable Nyquist Criterion to arrive at the sufficient condition for stability of the closed loop system. This sufficient condition leads to the introduction of a class of transfer function matrices, H_2, that stabilize the family of linearly treated robot manipulators. The detailed derivation for the stability condition is given in Appendix B. Appendix C shows that the stability condition given by Nyquist Criterion is a subset of the criteria given by the Small Gain Theorem. Using the results in Appendix B, the sufficient condition for stability is given by inequality 27.

$$\sigma_{max}(H_2)<\frac{1}{\sigma_{max}((S_1+S_2)^{-1}G_2)} \quad \forall\omega\in(0,\infty) \tag{27}$$

Similar to the nonlinear case, H_2 must be chosen such that its "size" is smaller than the reciprocal of the "size" of the forward loop mapping in Figure 7 to guarantee the stability of the closed loop system. Note that in inequality 27 σ_{max} represents a "size" of H_2 in the singular value sense.

* The maximum singular value of a matrix A, $\sigma_{max}(A)$ is defined as:

$$\sigma_{max}(A)=\max\frac{|Az|}{|z|}$$

where z is a non-zero vector and $|\cdot|$ denotes the Euclidean norm.

Consider $n=1$ (one degree of freedom system) for more understanding about the stability criterion. The stability criterion when $n=1$ is given by inequality 28.

$$|G_2H_2|<|S_1+S_2| \quad \forall\omega\in(0,\infty) \tag{28}$$

where $|\cdot|$ denotes the magnitude of a transfer function. Since in many cases $G_2\approx 1$ with the bandwidth of the tracking controller of each robot, ω_0, then H_2 must be chosen such that:

$$|H_2|<|S_1+S_2| \quad \forall\omega\in(0,\omega_0) \tag{29}$$

Inequality 29 reveals some facts about the size of H_2. The smaller the sensitivity functions of the robot manipulators are, the smaller H_2 must be chosen. In the "ideal case", no H_2 can be found to allow two perfect tracking robots ($S_1=S_2=0$) interact with each others. In other words, for the stability of the system shown in Figure 5, there must be some compliancy in either first or second robot. RRC, structural dynamics, and the tracking controller stiffness form the compliancy on the robot.

Suppose, the first robot is an ideal positioning system. In other words, S_1 has a zero gain. Therefore the contact force and the position of contact point between two robots are:

$$f_{2\infty}=(S_2+G_2H_2)^{-1}(G_1e_1-G_2r_2) \tag{30}$$

$$y_{1\infty}=G_1(e_1) \tag{31}$$

The first robot controls the position of the contact point, while the other controls the contact force. Generalizing this concept to n robots, one robot controls the position of the contact point while the other robots control the $n-1$ contact forces such that:

$$f_1+f_2+f_3+\cdots+f_n=0 \tag{32}$$

EXAMPLE

Consider two one-degree of freedom robots with G and S in equation (1) given as:

$$G_1(s)=\frac{0.85}{(s/5+1)(s/9+1)(s/190+1)(s/240+1)(s/290+1)}$$

$$G_2(s)=\frac{1}{(s/6+1)(s/10+1)(s/200+1)(s/250+1)(s/300+1)}$$

$$\frac{0.1}{(s/4+1)(s/8+1)} \qquad S_2(s)=\frac{0.05}{(s/5+1)(s/9+1)}$$

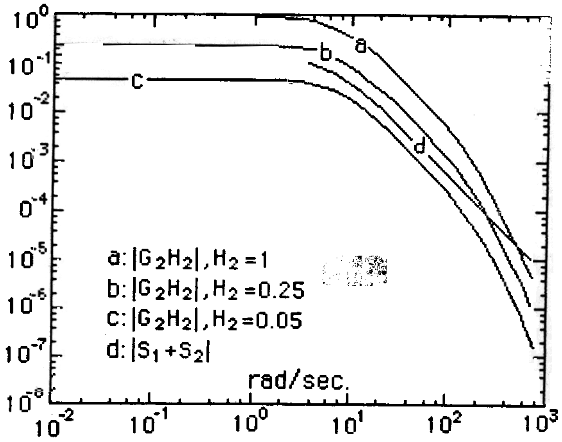

Fig. 8. $|G_2H_2| < |S_1 + S_2|$ is a sufficient condition for stability

Both robots have good positioning capability (small gain for S). The poles that are located at -250, -300, -290, -240 show the high frequency modes in the robots. The stability of the robots when they are in contact with each other is analyzed. If we consider H_2 as a constant gain, then inequality 28 yields that for $H_2 \leq 0.08$ the value of $|G_2H_2|$ is always smaller than $|S_1 + S_2|$ for all $\omega \in (0, \infty)$. Figure 8 shows the plots of $|G_2H_2|$ and $|S_1 + S_2|$ for three values of H_2. For $H_2 = 0.05$ the system is stable with the closed loop poles located at (-456.71, $-147.24 \pm 172.37j$, -9.41, -8.38, -5.62, -4.58) while $H_2 = 1$ results in unstable system with the closed loop poles located at (-800.88, -9.03, -8.05, -5.05, -4.13, $23.98 \pm 477.35j$). Note that the stability condition derived via inequality 28 is a sufficient condition for stability; many compensators can be found to stabilize the system without satisfying inequality 28. Figure 8 shows an example ($H_2 = 0.25$) that does not satisfy inequality 28 however the system is stable with closed loop poles at (-598.64, $-76.87 \pm 298.04j$, -9.1, -8.15, -5.19, -4.36). If one uses root locus for stability analysis, for $H_2 \leq 0.75$ all the closed loop poles will be in the left half plane. Once a constant value for stabilizing H_2 established, one can choose a dynamic compensator to filter out the high frequency noise in the force measurements.

CONCLUSION

A new architecture for compliance control of two cooperating robots has been investigated using unstructured models for dynamic behavior of robots. Each robot end-point follows its position input command vector "closely" when the robots are not in contact with each other. When two robots come in contact with each other, one robot controls the position of the contact point, while the other controls the contact force. The unified approach of modeling robots is expressed in terms of sensitivity functions. A bound for the global stability of the manipulators has been derived. For the stability of two robots, there must be some initial compliancy in either robot. The initial compliancy in the robots can be obtained by a non-zero sensitivity function for the tracking controller or a passive compliant element such as an RCC.

APPENDIX A

Definition 1 to 7 will be used in the stability proof of the closed-loop system (6, 7).

Definition 1: For all $p \in (1, \infty)$, we label as L_p^n the set consisting of all functions $f = (f_1, f_2, \dots, f_n)^T: (0, \infty) \mapsto \mathbb{R}^n$ such that:

$$\int_0^\infty |f_i|^p \, dt < \infty \quad \text{for} \quad i = 1, 2, \quad , n$$

Definition 2: For all $T \in (0, \infty)$, the function f_T defined by;

$$f_T = \begin{cases} f & 0 \leq t \leq T \\ 0 & T \leq t \end{cases}$$

is called the truncation of f to the interval (0, T).

Definition 3: The set of all function $f = (f_1, f_2, \dots, f_n)^T$: $(0, \infty) \mapsto \mathbb{R}^n$ such that $f_T \in L_p^n$ for all finite T is denoted by L_{pe}^n. f by itself or may not belong to L_p^n.

Definition 4: The norm on L_p^n is defined by;

$$\|f\|_p = \left(\sum_{i=1}^n \|f_i\|_p^2\right)^{1/2}$$

where $\|f_i\|_p$ is defined as

$$\|f_i\|_p = \left(\int_0^\infty w_i |f_i|^p \, dt\right)^{1/p}$$

where w_i is the weighting factor. w_i is particularly useful for scaling forces and torques of different units.

Definition 5: Let $V_2(\cdot)$: $L_{pe}^n \mapsto L_{pe}^n$. We say that the operator $V_2(\cdot)$ is L_p-stable, if:

a) $V_2(\cdot)$: $L_p^n \mapsto L_p^n$

b) there exist finite real constants α_2 and β_2 such that:

$$\|V_2(e_2)\|_p \leq \alpha_2 \|e_2\|_p + \beta_2 \quad \forall e_2 \in L_p^n$$

According to this definition we first assume that the operator maps L_{pe}^n to L_{pe}^n. It is clear that if one does not show that $V_2(\cdot)$: $L_{pe}^n \mapsto L_{pe}^n$, the satisfaction of condition (a) is impossible since L_{pe}^n contains L_p^n. Once the mapping of $V_2(\cdot)$ from L_{pe}^n to L_{pe}^n is established, then we say that the operator $V_2(\cdot)$ is L_p-stable if whenever the input belongs to L_p^n the resulting output belongs to L_p^n. Moreover, the norm of the output is not larger than α_2 times the norm of the input plus the offset constant β_2.

Definition 6: The smallest α_2 such that there exists a constant β_2 so that inequality b of Definition 5 is satisfied is called the gain of the operator $V_2(\cdot)$.

Definition 7: Let $V_2(\cdot)$: $L_{pe}^n \mapsto L_{pe}^n$. The operator $V_2(\cdot)$ is said to be causal if:

$$V_2(e_2)_T = V_2(e_{2T}) \forall T < \infty \quad \text{and} \quad \forall e_2 \in L_{pe}^n$$

PROOF OF THE NONLINEAR STABILITY PROPOSITION

Define the closed-loop mapping $A: (e_1, r_2) \mapsto e_2$ (Figure 6).

$$e_2 = r_2 + H_2(V_1(e_1) - V_2(e_2)) \quad \text{(A1)}$$

For each finite T, inequality A2 is true.

$$\|e_{2T}\|_p \leq \|r_{2T}\|_p + \|H_2(V_1(e_1) - V_2(e_2))_T\|_p \quad \forall T < \infty \quad \text{(A2)}$$

$H_2(V_1(e_1) - V_2(e_2))$ is L_p-stable, therefore, using inequalities 18, 19, and 21:

$$\|e_{2T}\|_p \leq \|r_{2T}\|_p + \alpha_3\alpha_1 \|e_{1T}\|_p + \alpha_3\alpha_2 \|e_{2T}\|_p + \alpha_3\beta_1 + \alpha_3\beta_2 + \beta_3 \quad \forall T < \infty \quad \text{(A3)}$$

Since $\alpha_3\alpha_2$ is less than unity:

$$\|e_{2T}\|_P \leq \frac{\|e_{1T}\|_p}{1-\alpha_3\alpha_2} + \frac{\|r_{2T}\|_p}{1-\alpha_3\alpha_2} + \frac{\alpha_3(\beta_1+\beta_2)+\beta_3}{1-\alpha_3\alpha_2} \quad \forall T < \infty \quad \text{(A4)}$$

Inequality A4 shows that $e_2(\cdot)$ is bounded over $(0, T)$. Because this reasoning is valid for every finite T, it follows that $e_2(\cdot) \in L^n_{pe}$, i.e., that $A: L^n_{pe} \mapsto L^n_{pe}$. Next we show that the mapping A is L_p-stable in the sense of Definition 5. Since $\|r_2\|_p$ and $\|e_1\|_p < \infty$ (they both belong to L^n_{pe} space), then from inequality A4:

$$\|e_{2T}\|_P < \infty \quad \forall T < \infty \quad \text{(A5)}$$

In the limit when $T \to \infty$:

$$\|e_2\|_P < \infty \quad \text{(A6)}$$

Inequality A6 implies e_2 belongs to L^n_p-space whenever r_2 and e_1 belong to L^n_p-space. With the same reasoning from equation (A1) to (A5), it can be shown that inequality (A7) is true.

$$\|e_2\|_P \leq \frac{\|e_1\|_p}{1-\alpha_3\alpha_2} + \frac{\|r_2\|_p}{1-\alpha_3\alpha_2} + \frac{\alpha_3(\beta_1+\beta_2)+\beta_3}{1-\alpha_3\alpha_2} \quad \text{(A7)}$$

Inequality (A7) shows the linear boundedness of e_2. (Condition b of Definition 5). Inequality (A7) and (A6) taken together, guarantee that the closed-loop mapping A is L_p-stable.

APPENDIX B

The objective is to find a sufficient condition for stability of the closed-loop system in Figure 7 by Nyquist Criterion. The block diagram in Figure 7 can be reduced to the block diagram in Figure B1 when all the operators are linear transfer function matrices.

There are two elements in the feedback loop; $G_2H_2S_1^{-1}$ and $S_2S_1^{-1} \cdot S_2S_1^{-1}$ shows the natural force feedback while $G_2H_2S_1^{-1}$ represents the controlled force feedback in the system. The objective is to use Nyquist Criterion[8] to arrive at the sufficient condition for stability of the system when $H_2 = 0$. The following conditons are noted:

1) The closed loop system in Figure B1 is stable if $H_2 = 0$. This condition simply states the stability of two robot manipulators. (Figure 4 shows this configuration.)
2) H_2 is chosen as a stable linear transfer function matrix. Therefore the augmented loop transfer function $(G_2H_2S_1^{-1} + S_2S_1^{-1})$ has the same number of unstable poles that $S_2S_1^{-1}$ has. Note that in many cases $S_2S_1^{-1}$ is a stable system.
3) Number of poles on $j\omega$ axis for both loops $S_2S_1^{-1}$ and $(G_2H_2S_1^{-1} + S_2S_1^{-1})$ are equal.

Considering that the system in Figure B1 is stable when $H_2 = 0$ we plan to find how robust the system is when $G_2H_2S_1^{-1}$ is added to the feedback loop. If the loop transfer function $S_2S_1^{-1}$ (without compensator, H_2) develops a stable closed-loop system, then we are looking for a condition on H_2 such that the augmented loop transfer function $(G_2H_2S_1^{-1} + S_2S_1^{-1})$ guarantees the stability of the closed-loop system. According to the Nyquist Criterion, the system in Figure B1 remains stable if the anti-clockwise encirclement of the $\det(G_2H_2S_1^{-1} + S_2S_1^{1} + I_n)$ around the center of the s-plane is equal to the number of unstable poles of the loop transfer function $(G_2H_2S_1^{-1} + S_2S_1^{-1})$. According to conditions 2 and 3, the loop transfer functions $S_2S_1^{-1}$ and $(G_2H_2S_1^{-1} + S_2S_1^{-1})$ both have the same number of unstable poles. The closed-loop system when $H_2 = 0$ is stable according to condition 1; the encirclements of $\det(S_2S_1^{-1} + I_n)$ is equal to unstable poles of $S_2S_1^{-1}$. Since the number of unstable poles of $(G_2H_2S_1^{-1} + S_2S_1^{-1})$ and that of $S_2S_1^{-1}$ are the same, therefore for stability of the system $\det.(G_2H_2S_1^{-1} + S_2S_1^{-1} + I_n)$ must have the same number of encirclements that $\det.(S_2S_1^{-1} + I_n)$ has. A sufficient condition to guarantee the equality of the number of encirclements of $\det(G_2H_2S_1^{-1} + S_2S_1^{-1} + I_n)$ and that of $\det(S_2S_1^{-1} + I_n)$ is that the $\det.(G_2H_2S_1^{-1} + S_2S_1^{-1} + I_n)$ does not pass through the origin of the s-plane for all possible non-zero but finite values of H_2, or

$$\det(G_2H_2S_1^{-1} + S_2S_1^{-1} + I_n) \neq 0 \quad \forall \omega \in (0, \infty) \quad \text{(B1)}$$

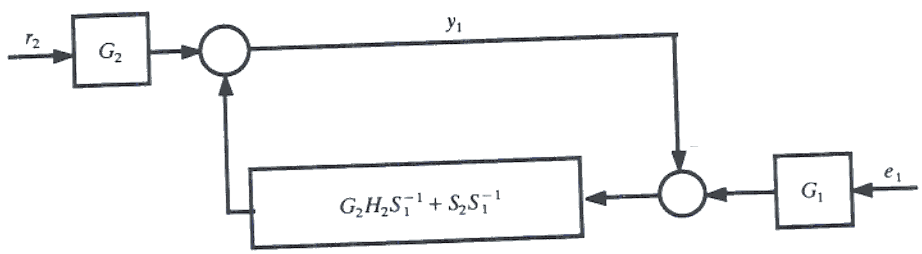

Fig. B1. Simplified block diagram of the system in Figure 7.

If inequality B1 does not hold then there must be a non-zero vector z such that:

$$(G_2H_2S_1^{-1} + S_2S_1^{-1} + I_n)z = 0 \quad \text{(B2)}$$

or

$$G_2H_2S_1^{-1}z = -(S_2S_1^{-1} + I_n)z \quad \text{(B3)}$$

A sufficient condition to guarantee that equality B3 will not happen is given by inequality B4.

$$\sigma_{\max}(G_2H_2S_1^{-1}) < \sigma_{\min}(S_2S_1^{-1} + I_n) \quad \forall\omega \in (0, \infty) \quad \text{(B4)}$$

or a more conservative condition;

$$\sigma_{\max}(H_2) < \frac{1}{\sigma_{\max}((S_1+S_2)^{-1}G_2)} \quad \forall\omega \in (0, \infty) \quad \text{(B5)}$$

Note that $(S_1 + S_2)^{-1}G_2$ is the transfer function matrix that maps e_2 to the contact force, f_2 when $e_1 = 0$. Figure 7 shows the closed-loop system. According to the result of the proposition, H_2 must be chosen such that the size of H_2 is smaller than the reciprocal of the size of the forward loop transfer function, $(S_1 + S_2)^{-1}G_2$.

APPENDIX C

The following inequalities are true when $p = 2$ and H_2 and V_2 are linear operators.

$$\|H_2(f_2)\|_p \leq \|f_2\|_p \quad \text{(C1)}$$

$$\|V_2(e_2)\|_p \leq \mu \, \|e_2\|_p \quad \text{(C2)}$$

where:

$\mu = \sigma_{\max}(Q)$, and Q is the matrix whose ijth entry is given by $(Q)_{ij} = \sup_\omega |(V_2)_{ij}|$,

$\nu = \sigma_{\max}(R)$, and R is the matrix whose ijth entry is given by $(R)_{ij} = \sup_\omega |(H_2)_{ij}|$

According to the stability condition, to guarantee the closed loop stability $\mu\nu < 1$ or:

$$\nu < \frac{1}{\mu} \quad \text{(C3)}$$

Note that the following are true;

$$\sigma_{\max}(V_2) \leq \mu \quad \forall\omega \in (0, \infty) \quad \text{(C4)}$$

$$\sigma_{\max}(H_2) \leq \nu \quad \forall\omega \in (0, \infty) \quad \text{(C5)}$$

Substituting C4 and C5 inequality C3 which guarantees the stability of the system, the following inequality is obtained;

$$\sigma_{\max}(H_2) < \frac{1}{\sigma_{\max}(V_2)} \quad \forall\omega \in (0, \infty)$$

$$\sigma_{\max}(H_2) < \frac{1}{\sigma_{\max}((S_1+S_2)^{-1}G_2)} \quad \forall\omega \in (0, \infty) \quad \text{(C7)}$$

Inequality C7 is identical to inequality 27. This shows that the linear stability condition by the multivariable Nyquist Criterion is a subset of the general stability condition given by the Small Gain Theorem.

References

1. H. Kazerooni, T.B. Sheridan and P.K. Houpt, "Robust Complaint Motion for Manipulators, Part I: The Fundamental Concepts of Compliant Motion", *IEEE J. Robotics and Automation* **2,** No. 2, 83–92 (June, 1986).
2. H. Kazerooni, T.B. Sheridan and P.K. Houpt, "Robust Compliant Motion for Manipulators, Part II: A Design Method" *IEEE J. Robotics and Automation* **2,** No. 2, 93–105 (June, 1986).
3. H. Kazerooni, "Direct Drive Active Compliant End-Effector (Active RCC)" *IEEE J. Robotics and Automation* **4,** No. 3, 324–333 (June, 1988).
4. H. Kazerooni and T.I. Tsay, "On the Stability of the Robot Compliant Motion Control" **In:** *Proceedings of the IEEE Robotics and Automation Conference, Philadelphia, PA* **2.** 1166–1172 (April, 1988).
5. M.W. Spong and M. Vidyasagar, "Robust Nonlinear Control of Robot Manipulators" *IEEE Conference on Decision and Control* **3,** 1767 (December, 1985).
6. M. Vidyasagar, *Nonlinear Systems Analysis* (Prentice-Hall: Englewood Cliffs, New Jersey, 1978).
7. M. Vidyasagar and C. A. Desoer, *Feedback Systems: Input–Output Properties,* (Academic Press New York, NY, 1975).
8. N.A. Lehtomaki, N.R. Sandell and M. Athans, "Robustness Results in Linear-Quadratic Gaussian Based Multivariable Control Designs" *IEEE Transaction on Automatic Control* **AC26,** No. 1, 75–92 (February, 1981).